The Conserved Core Domains of Annexins A1, A2, A5, and B12 Can Be Divided into Two Groups with Different Ca^{2+}-Dependent Membrane-Binding Properties†

Darshana R. Patel,‡ J. Mario Isas,‡,§ Alexey S. Ladokhin,|| Christine C. Jao,‡ Yujin E. Kim,§ Thorsten Kirsch,⊥ Ralf Langen,§ and Harry T. Haigler*,‡

Department of Physiology and Biophysics, University of California, 19172 Jamboree, Irvine, California 92697, Department of Biochemistry and Molecular Biology, University of Southern California, Los Angeles, California 90033, Department of Biochemistry and Molecular Biology, The University of Kansas Medical Center, Kansas City, Kansas 66160-7421, and Musculoskeletal Research Laboratories, Department of Orthopaedics, University of Maryland School of Medicine, Baltimore, Maryland 21201

Received November 5, 2004; Revised Manuscript Received December 15, 2004

ABSTRACT: The hallmark of the annexin super family of proteins is Ca^{2+}-dependent binding to phospholipid bilayers, a property that resides in the conserved core domain of these proteins. Despite the structural similarity between the core domains, studies reported herein showed that annexins A1, A2, A5, and B12 could be divided into two groups with distinctively different Ca^{2+}-dependent membrane-binding properties. The division correlates with the ability of the annexins to form Ca^{2+}-dependent membrane-bound trimers. Site-directed spin-labeling and Förster resonance energy transfer experimental approaches confirmed the well-known ability of annexins A5 and B12 to form trimers, but neither method detected self-association of annexin A1 or A2 on bilayers. Studies of chimeras in which the N-terminal and core domains of annexins A2 and A5 were swapped showed that trimer formation was mediated by the core domain. The trimer-forming annexin A5 and B12 group had the following Ca^{2+}-dependent membrane-binding properties: (1) high Ca^{2+} stoichiometry for membrane binding (∼12 mol of Ca^{2+}/mol of protein); (2) binding to membranes was very exothermic (> −60 kcal/ mol of protein); and (3) binding to bilayers that were in the liquid-crystal phase but not to bilayers in the gel phase. In contrast, the nontrimer-forming annexin A1 and A2 group had the following Ca^{2+}-dependent membrane-binding properties: (1) lower Ca^{2+} stoichiometry for membrane binding (≤4 mol of Ca^{2+}/mol of protein); (2) binding to membranes was relatively less exothermic (< −33 kcal/ mol of protein); and (3) binding to bilayers that were in either the liquid-crystal phase or gel phase. The biological implications of this subdivision are discussed.

Annexins are a super family of proteins that typically bind with high affinity to phospholipid bilayers in a reversible Ca^{2+}-dependent manner (*1*). Annexins have been implicated in a number of intracellular membrane-related events such as vesicular trafficking and fusion (*2, 3*), but their exact biological functions have not been clearly defined. Although annexins are primarily intracellular proteins involved in Ca^{2+} signaling, atypical properties have been described including extracellular localization (*3*, *4*) and Ca^{2+}-independent membrane association (*5*−*8*). Because annexins A1, A2, and A5 have been implicated in human diseases (*9*−*11*), a more complete understanding of their structure and function may have medical implications.

Annexins are not found in yeasts and prokaryotes, but 100's of annexin genes are expressed in vertebrates (the "A" family), invertebrates (the "B" family), plants (the "D" family), and other eukaryotes (*1*). Mammals have 12 annexin genes (annexin A1, annexin A2, etc.), and several different annexins tend to be expressed in each cell type (*1*). The functional rationale for this complex and overlapping expression pattern of these closely related proteins is an intriguing mystery. Annexins have a structurally conserved core domain that contains the Ca^{2+}-binding sites and a nonconserved N-terminal domain that often contains phosphorylation sites (*1*). Speculation regarding the physiological need for such a vast array of annexin gene products often proposes specialized functions for individual annexins and implicates the unique N-terminal domain in the function. However, it is also possible that the core domain plays a direct role in annexin biology that extends beyond binding to cellular membranes in response to Ca^{2+} signals. We now report a study of the Ca^{2+}-dependent membrane-binding properties of annexins A1, A2, A5, and B12 designed to search for similarities and differences in the highly conserved core domains of annexins.

† This work was supported by National Institutes of Health Grants GM55651 (to H.T.H.), GM63915 (to R.L.), AR46245 (to T.K.), GM069783 (to A.S.L.) and GM07311 (predoctoral training grant to D.R.P.) and the Arthritis Foundation (to T.K.).

* To whom correspondence should be addressed: Department of Physiology and Biophysics, University of California, Irvine, CA 92697. Telephone: 949-824-6304. Fax: 949-824-8540. E-mail: hhaigler@uci.edu.

‡ Department of Physiology and Biophysics, University of California, Irvine, CA 92697.

§ Department of Biochemistry and Molecular Biology, University of Southern California, Los Angeles, CA 90033.

|| Department of Biochemistry and Molecular Biology, The University of Kansas Medical Center, Kansas City, KS 66160-7421.

⊥ Musculoskeletal Research Laboratories, Department of Orthopaedics, University of Maryland School of Medicine, Baltimore, MD 21201.

10.1021/bi047642+ CCC: $30.25 © 2005 American Chemical Society
Published on Web 02/02/2005

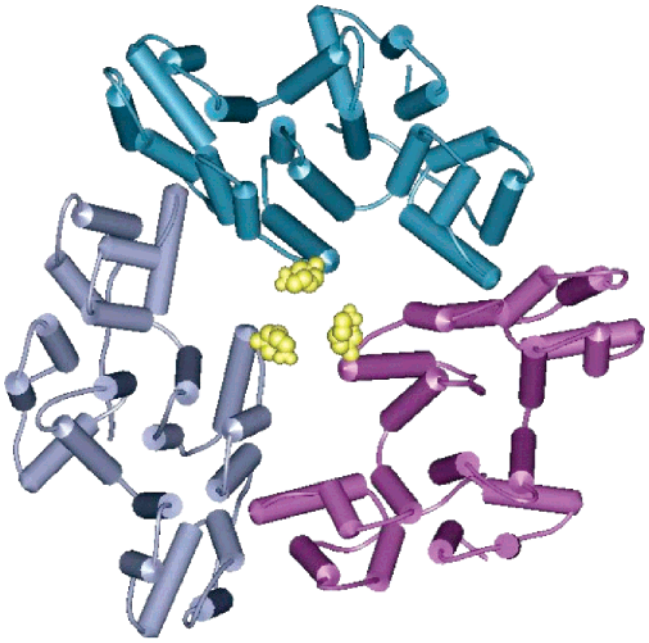

FIGURE 1: Crystal structure of annexin B12 trimer. Each monomer of the annexin B12 trimer is illustrated with a different color. The side chain of residue 132 is shown in yellow.

The core domains of annexins consist of four structurally conserved repeats that are ~70 amino acids long (*7*). High-resolution crystal structures of the soluble forms of many different annexins are all nearly superimposable and reveal that each of the four repeats consists of a bundle of four α helices with an additional helix sitting on top (Figure 1). Two short connecting loops on the bottom of each four-helix bundle are involved in the formation of Ca^{2+}-binding sites (*12*, *13*). Trimers have been observed in crystal structures of annexin B12 (*14*) (illustrated in Figure 1) and in some of the crystal structures of annexin A5 (*15*). Trimers have not been observed in crystal structures of annexins A1 and A2. Despite the high-resolution information on the structure of soluble annexins, the structure of the biologically relevant membrane-bound form has not been determined at high resolution. Low-resolution electron microscopic images of mammalian annexins A4 and A5 indicated that these proteins formed trimers on monolayers and that the general shape of the membrane-bound protein was similar to the crystal structures of the soluble proteins (*16*, *17*). Atomic force microscopic studies of annexin A5 drew the same conclusions (*18*).

We recently have used the site-directed spin-labeling (SDSL)[1] experimental approach to focus on hydra annexin B12 as a model for the structure and function of membrane-bound animal annexins (*5*, *8*, *12*, *19*, *20*). The strategy involved site-directed mutagenesis to introduce a single-cysteine residue that was subsequently modified with a thiol-reactive nitroxide reagent to generate the spin-labeled side chain designated R1 (see Figure 2). The electron paramagnetic resonance (EPR) spectrum of R1 attached to the protein is sensitive to the environment of the nitroxide (*21*, *22*).

[1] Abbreviations: DMPS, dimyristoyl phosphatidylserine; DTPC, ditridecanoyl phosphatidylcholine; EPR, electron paramagnetic resonance; FRET, Förster resonance energy transfer, ITC, isothermal titration calorimetry; PC, phosphatidylcholine; PS, phosphatidylserine SDSL, site-directed spin labeling.

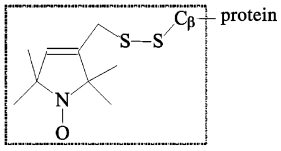

FIGURE 2: Structure of R1 side chain.

Nitroxide scans through extended regions of annexin B12 showed that it had the same general backbone fold in solution and in the Ca^{2+}-dependent membrane-bound state (*12*, *20*). We also studied the quaternary state of annexin B12 by exploiting the fact that, when R1 side chains are in close proximity, spin−spin interactions occur that can serve as molecular rulers to measure distances up to ~25 Å using continuous wave EPR (*19*). This phenomenon was used to measure trimer formation by placing a single R1 side chain at residue 132 near the 3-fold axis of the annexin B12 crystallographic trimer (Figure 1). Dramatic EPR spectral differences were observed when the soluble monomer assembled into a trimer on the surface of phospholipid vesicles in the presence of Ca^{2+}. In contrast to other methods used to date, the SDSL approach quantitatively determines the percent of membrane-bound annexin that forms trimers. In this paper, we used EPR analysis to evaluate trimer formation of annexins A1, A2, and A5 mutants that were labeled with R1 at single-cysteine residues at positions homologous to position 132 in annexin B12. We also labeled the same cysteine residues in annexins A1, A2, A5, and B12 with donor and acceptor fluorescence dyes and then evaluated self-association using Förster resonance energy transfer (FRET) experiments, a molecular ruler capable of detecting interactions involving distances over 2-fold longer than those detected by continuous-wave EPR. These SDSL and FRET experiments confirm the trimer-forming ability of human annexin A5 and hydra B12 and directly demonstrate their ability to form heterotrimers. Because the two proteins are not orthologues, trimer formation must be an archetypal function of annexins that was highly conserved in certain annexin gene products. In contrast, no evidence of self-association of annexins A1 and A2 was detected.

Because some annexins form trimers and some do not, we asked whether there were differences in the Ca^{2+}- and phospholipid-binding properties that correlated with this property. Annexins appear to bind to bilayers by a "Ca^{2+} bridge" mechanism in which oxygen atoms on the protein and oxygen atoms in the headgroups of bilayer phospholipids jointly coordinate the bridging Ca^{2+} (*12*, *13*, *23*). Most models envision Ca^{2+}-dependent membrane being mediated primarily by a "type II" Ca^{2+}-binding site in each 70 amino acid repeat (*2*). However, reports of the number of Ca^{2+} sites involved in annexin binding vary widely. Recently, we carefully evaluated the Ca^{2+} stoichiometry for annexin B12 and reported ~12 mol of Ca^{2+}/mol of protein for binding to bilayers (*24*). We proposed a model in which there is complimentarity between the spacing of the Ca^{2+}-binding sites and the spacing of the phospholipid headgroups in bilayers (*24*). Changing the spacing of the headgroups of bilayers by undergoing a gel-phase transition in response to cooling prevented the binding of annexin B12. In this paper, we further explore this model and show that the stoichiometry of Ca^{2+} binding and headgroup spacing-dependent binding of annexin A5 resembles that of annexin B12. In contrast,

the Ca^{2+}-binding stoichiometry was much lower for annexins A1 and A2, and they were able to bind with high affinity to phospholipid bilayers that were in the gel phase. These studies show that annexins A1, A2, A5, and B12 can be grouped into two pairs with distinctively different Ca^{2+}-dependent phospholipid-binding properties. This may be a first step toward defining groupings of annexins with distinctive functional properties that reside in the conserved core domains.

EXPERIMENTAL PROCEDURES

Materials. The Ca^{2+} source for stoichiometry experiments was $CaCl_2$ standard from Thermo Orion (Beverly, MA). The spin-label (1-oxyl-2,2,5,5-tetramethylpyrroline-3-methyl) methanethiosulfonate was purchased from Toronto Research Chemicals. Alexa Fluor 532 C_5 maleimide (A-10265) and Alexa Fluor 647 C_2 maleimide (A-20347) were obtained from Molecular Probes (Eugene, OR).

Annexin Expression and Purification. Site-directed mutagenesis by the Clontech method (Palo Alto, CA) was used to replace native cysteine 316 with Ala (C316A) in the pSE420 plasmid of human *ANX5*. A single cysteine was then introduced into C316A by replacing glycine 134 with cysteine. Site-directed mutagenesis by the Clontech method was used to remove all cysteines (C9S, C133A, C262A, and C335A) encoded by the human *ANX2* pSE420 plasmid (provided by V. Gerke). A single cysteine was introduced into position 152 (K152C) of cysteine-less annexin A2 by the Clontech method. Site-directed mutagenesis by the Clontech method was used to remove all five native cysteines (C263A, C270A, C314A, C324A, and C343A) encoded by the porcine *ANX1* pSE420 plasmid (provided by V. Gerke). A single cysteine was then introduced at position K161 of cysteine-less *ANX1* by the Stratagene method.

The cysteine-less and single-cysteine mutants of annexins A2 and A5 were expressed in recombinant bacteria and purified by reversible Ca^{2+}-dependent binding to phospholipid vesicles followed by column chromatography by previously published protocols for annexin B12 (*24*). Cysteine-less and single-cysteine mutants of annexin A1 were expressed in recombinant bacteria and purified by column chromatography in the presence of ethylene glycol bis(2-aminoethyl ether)-*N*,*N*,*N*′,*N*′-tetraacetic acid (EGTA) by a previously described method (*25*). All annexin concentrations were determined by absorbance at 280 nm with the following extinction coefficients: annexin A1 ϵ_{280}, 20 010 M^{-1} cm^{-1}; annexin A2 ϵ_{280}, 30 250 M^{-1} cm^{-1}; annexin A5 ϵ_{280}, 21 110 M^{-1} cm^{-1}; and annexin B12 ϵ_{280}, 12 288 M^{-1} cm^{-1}. Purified proteins were stored in the presence of dithiothreitol (2 mM) at −70 °C in the final buffer used in the purification, with the exception of annexin A2, which was stored at −20 °C in MES buffer (20 mM, pH 6.5) containing 25% glycerol and dithiothreitol (2 mM).

Construction and Expression of Chimeras of Annexins A2 and A5. Previously described cDNA clones of chicken annexins A2 and A5 (*26*) were used to construct chimeric annexin A2/A5 molecules in which the N-terminal and core domains were swapped. A chimera containing the N-terminal domain of annexin A2 and the core domain of annexin A5 (called "2N-terminal:5core") was created from the annexin A2 fragment encoding the N-terminal domain (amino acids 2−37) and the annexin A5 fragment encoding the core region of annexin A5 (amino acids 20−322) that were prepared by polymerase chain reaction (PCR) using appropriate primers. The 5′ primer for the annexin A5 fragment was extended at the 5′ end to provide a codon (GAT), which encodes Asp present in annexin A2 at position 38, and to provide a site for cleavage with *Msp*I without altering the amino acid sequence. The annexin A2 and A5 fragments were cleaved with *Msp*I and then ligated to each other. The resulting ligation product was cleaved at the *Bam*HI sites and ligated to *Bam*HI-digested pGEX expression vector (Pharmacia). For the construction of the chimeric protein called "5N-terminal:2core" containing the N-terminal domain of annexin A5 (amino acids 2−12) and the core domain of annexin A2 (amino acids 31−340), a 5′ primer encoding the N-terminal domain sequence of annexin A5 (amino acids 2−12) and the N-terminal sequence of annexin A2 core domain was constructed. The "5N-terminal:2core" chimera was prepared by PCR using the above-mentioned 5′ primer and a 3′ primer encoding the C-terminal annexin A2 core domain. The resulting PCR product was cloned into pGEX vector. Both constructs were confirmed by nucleotide sequencing.

Recombinant annexin chimeras were expressed and purified using the pGEX expression vector as described previously (*27*). Briefly, recombinant annexin−GST fusion protein was expressed in *Escherichia coli* DH5αF′ and purified by affinity chromatography. The fusion protein was subjected to PreScission protease (Pharmacia) cleavage to release the annexin molecules from the GST moiety. The reversible Ca^{2+}-dependent binding of annexin to phosphatidylserine (PS)-containing liposomes was used as an affinity purification step to remove bacterial contaminants. One preparation of each chimera also underwent an additional final purification step involving ion-exchange FPLC chromatography.

Preparation of Phospholipid Vesicles. The following preparations of lipids were obtained from Avanti Polar Lipids (Alabaster, AL) and were used to make large unilammelar vesicles by the method of Reeves and Dowben (*28*): phosphatidylserine (PS, brain, catalog number 840032) and phosphatidylcholine (PC, egg yolk, catalog number 840051). In certain experiments, vesicles were prepared from phospholipids with saturated acyl chains: dimyristoyl phosphatidylserine (DMPS, 14:0, catalog number 840033) and ditridecanoyl phosphatidylcholine (DTPC, 13:0, catalog number 850340). The Ca^{2+} source for stoichiometry experiments was the $CaCl_2$ standard from Thermo Orion (Beverly, MA).

SDSL of Single-Cysteine Annexin Mutants. Size-exclusion chromatography with P-10 columns was used to remove dithiothreitol from the buffer in which the isolated single-cysteine proteins were stored. Immediately thereafter, the cysteine-specific spin-label (1-oxyl-2,2,5,5-tetramethylpyrroline-3-methyl) methanethiosulfonate (3-fold molar excess) was added and incubated in HEPES buffer (20 mM, pH 7.4) containing 100 mM NaCl for 2 h at room temperature. After unreacted reagent was removed by size-exclusion chromatography (P-10 columns), proteins were concentrated by use of Amicon Microcon (Millipore, Bedford, MA). Spin-labeled mutants of annexins are designated by giving the sequence position of the cysteine substitution followed by the code for the nitroxide spin label, R1.

EPR Spectroscopy. EPR experiments were performed by adding spin-labeled annexin mutants (∼5 μg of protein) to

buffer (20 mM HEPES and 100 mM NaCl at pH 7.4) or to buffer containing phospholipid vesicles (lipid/protein molar ratio of 500:1). In most experiments, the annexins were induced to bind to the vesicles by the addition of 1 mM Ca^{2+}. For the determination of spin−spin interactions of annexins in trimer complexes, labeled and unlabeled ANXs were combined as follows: 5 μg of 161R1 annexin A1 or 152R1 annexin A2 was diluted 1:1 with cysteine-less annexin, whereas 5 μg of 134R1 annexin A5 or 132R1 annexin B12 was diluted 1:5 with cysteine-less annexins. Annexins were mixed with vesicles, and then binding was induced by adding Ca^{2+} (1 mM). The lipid/protein molar ratio remained at 500:1.

The chimeric proteins were evaluated for their ability to form heterotrimers with annexins A5 and B12 as follows. 134R1 annexin A5 (10 μg) or 132R1 annexin B12 (10 μg) was mixed with either "5N-terminal:2core" (40 μg) or "2N-terminal:5core" (40 μg) and then added to phospholipid vesicles (lipid/protein molar ratio of 600:1) in the presence of Ca^{2+} (1 mM) in the buffer described above.

X-band EPR spectra were obtained using a Bruker EMX spectrometer fitted with a ER4119 HS cavity. All spectra were recorded at 2 mW incident microwave power using a field modulation of 1.5 G at 100 kHz and are presented with a spectral breadth of 100 G.

Fluorescence. Labeling of single-cysteine annexin mutants with Alexa 532 and Alexa 647 dyes was performed using a standard procedure for the thiol-reactive maleimide derivatives (*29*). Typically 1 mg of maleimade derivative of the dye was dissolved into a 0.2−0.4 mL of 50 μM solution of protein in 10 mM HEPES at pH 7.0, containing 50 mM KCl, 1 mM ethylenediaminetetraacetic acid (EDTA), and 3mM NaN_3. The reaction mixture was incubated overnight at 4 °C. The excess of dye was removed by gel-filtration chromatography (PD-10 column) followed by a series of centrifugations using a Microcon YM-10 concentrator. Typically after several (5−7) runs, the solution coming through the concentrator did not contain any dye as assayed by absorbance spectroscopy. The concentration of labeled annexin was estimated from peak absorbance measurements and assuming that the extinction coefficients are the same as for the free dyes: 75 000 M^{-1} cm^{-1} for Alexa 532 and 265 000 M^{-1} cm^{-1} for Alexa 647.

Fluorescence experiments were performed on samples that contained 5 nM annexin labeled with the donor dye (Alexa 532), 10 nM annexin labeled with acceptor dye (Alexa 647), and 0.1 mM phospholipid vesicles made of 2:1 (w/w) mixture of bovine brain PS and egg yolk PC (PS/PC) in HEPES buffer (20 mM HEPES at pH 7.4) containing 100 mM KCl and 1 mM EDTA. Membrane binding was initiated by addition of small aliquots of a concentrated solution of Ca^{2+} to the final concentration of 0.5 mM Ca^{2+} in excess EDTA.

Fluorescence was measured using a SLM 8100 steady-state fluorescence spectrometer (Jobin Yvon, Edison, NJ, formerly SLM/AMINCO, Urbana, IL) equipped with double-grating excitation and single-grating emission monochromators. The measurements were made in 4 × 10 mm cuvettes oriented with the long axis parallel to the excitation beam. Temperature was maintained at 25 °C using a circulating water bath. Cross orientation of polarizers was used (excitation polarization set to vertical and emission polarization set to horizontal) to minimize the scattering contribution from vesicles and to eliminate spectral polarization effects in monochromator transmittance (*30*). Fluorescence excitation spectra of dye-labeled annexins were obtained by averaging 5−10 scans collected over a 470−660 nm range using 1 nm steps. The emission monochromator was set at 680 nm. Excitation slits were 8 nm, and emission slits were 16 nm.

Because of the spectral overlap of emission of Alexa 532 and absorbance of Alexa 647, these dyes could be used as a donor−acceptor pair in FRET experiments. The Förster distance R_o for this pair is ∼60 Å (Ladokhin, A. S., and Haigler H. T., *Biochemistry*, in press). Data are normalized at 647 nm to account for variation in the quantum yield of the acceptor. The complete details of spectroscopic analysis are the subject of a separate publication (Ladokhin, A. S., and Haigler H. T., *Biochemistry*, in press).

Copelleting Assay. Unless otherwise indicated, the standard copelleting assay contained phospholipid vesicles equilibrated in HEPES buffer (20 mM, pH 7.4, containing 100 mM NaCl) with the indicated concentration of $CaCl_2$. After incubation for 15 min with the indicated amount of annexin at 25 °C, the vesicles were centrifuged (16000*g*, for 5 min). Pellets including bound protein were separated from the supernatant containing unbound protein for further analysis.

A modification of the standard copelleting assay was used to quantify the stoichiometry of $^{45}Ca^{2+}$ binding to membrane-bound annexins as previously reported (*24*). Briefly, this assay contained annexin (50 μg) and vesicles (1:5 ratio of protein/phospholipid by weight) in a 1 mL final volume with the indicated Ca^{2+} concentration. The specific activity of the $^{45}Ca^{2+}$ in each sample was 1.1−1.4 nCi/nmole. After centrifugation, the pellets and supernatants were subjected to liquid scintillation counting to determine the total $^{45}Ca^{2+}$ bound to the vesicles. The pellets of parallel samples were analyzed to determine the amount of annexin in the pellet, and the Ca^{2+}-binding data were expressed as moles of Ca^{2+} per mole of annexin in the pellet. The concentration of Ca^{2+} used in the assay induced binding of ∼95% of the added annexin.

A second modification of the copelleting assay involved vesicles containing saturated phospholipids instead of phospholipids from a biological source, as described previously (*24*). Vesicle composed of equal amounts DTPC and DMPS (see above) were incubated with 10 μg of annexin A1, A2, or A5. All samples are at a 1:400 protein/lipid molar ratio and were incubated and centrifuged at the indicated temperature, with saturating Ca^{2+} for each (100 μM for annexin A1, 50 μM for annexin A2, and 150 μM for annexin A5), according to the standard copelleting assay described above. Duplicate samples were analyzed, and the percentage of added annexin that was associated with the pellet is shown along with the standard deviation. The phospholipid-phase transition temperature range was determined experimentally by differential-scanning calorimetry in the same buffer.

Isothermal Titration Calorimetry (ITC). ITC experiments were performed on an ultrasensitive Microcal MCS-ITC (Microcal, Inc., Northampton, MA) as previously described (*24*). Briefly, all components in the system were exchanged into thoroughly degassed HEPES buffer (100 mM, pH 7.5). The 1.37 mL sample cell, equilibrated to 25 °C, contained 25 μM annexin and phospholipid vesicles (2:1 PS/PC, 10 mg). A motorized titration syringe was used to add 5 μL aliquots of $CaCl_2$ (5 mM) to the sample cell. A total of 32

injections were made at 400 s intervals while stirring at 400 rpm. The rate of heat released after each injection of Ca^{2+} into the sample was measured and subsequently analyzed on Origin 5.0 software. Control experiments were performed to quantify the enthalpy of the interaction of Ca^{2+} with vesicles; i.e., Ca^{2+} was titrated into a sample cell containing buffer and vesicles in the absence of protein. This small value was subtracted from the values obtained in the presence of annexins.

RESULTS

Determination of Trimer Formation by SDSL. Previous studies with the 132R1 mutant of annexin B12 showed that spin−spin coupling between nitroxide side chains located near the 3-fold axis of the annexin B12 trimer was an effective approach to monitor Ca^{2+}-dependent trimer formation on membranes (*19*). Experiments described below have extended this experimental approach to annexins A1, A2, and A5 to evaluate their ability to self-associate on membranes. The native cysteine residues from each of these proteins were mutated to either alanine or serine, and single-cysteine residues then were introduced (see the Experimental Procedures) into the loop between the C and D helices, a site near the 3-fold axis in crystallographic trimers of annexins A5 and B12. The "Cys-less" annexins and single-cysteine mutants (161Cys annexin A1, 152Cys annexin A2, and 134Cys annexin A5) were expressed in recombinant bacteria and isolated as described in the Experimental Procedures. In copelleting assays these recombinant Cys-less and single-Cys annexins bound to phospholipid vesicles in a similar Ca^{2+}-dependent manner as their respective wild-type counterparts (data not shown).

The EPR spectra for 161R1 annexin A1, 152R1 annexin A2, and 134R1 annexin A5 are shown in Figure 3 in solution and following Ca^{2+}-dependent binding to vesicles composed of PS and PC (PS/PC, 2:1 molar ratio). For comparison, spectra for 132R1 annexin B12 also are shown. As seen in the first row of Figure 3, all four spin-labeled annexins have very similar EPR spectra in solution. In solution, all of the proteins had line shapes with sharp central resonance lines, as would be expected for a mobile nitroxide side chain on a loop exposed to the aqueous solution. The second row in Figure 3 shows the EPR line shapes for the spin-labeled annexins after binding to phospholipid vesicles in the presence of Ca^{2+}. The spectra for membrane-bound 161R1 annexin A1 and 152R1 annexin A2 (second row of Figure 3) were similar to those in solution except for a slight broadening of the spectral line width in the membrane-bound state, which would be expected to occur when protein tumbling was reduced upon membrane binding. The spectral line width also could be broadened in the membrane-bound state because of a subtle ordering of structure caused by the backbone fold becoming more rigid. Although subtle changes were observed upon membrane binding, there clearly was no evidence for spin−spin coupling in either the annexin A1 or A2 spectra. Relative to their spectra in solution, the spectra for membrane-bound 134R1 annexin A5 and 132R1 annexin B12 had spectral broadening and dramatic decreases in the spectral amplitude. These data indicate strong spin−spin coupling between nitroxides that are in close proximity in a trimer. Furthermore, the lack of a sharp signal in the center line of the EPR spectra of 134R1 annexin A5 and 132R1 annexin B12 indicate that trimer formation was nearly quantitative. On the basis of a detailed analysis of 132R1 annexin B12, we estimated that over 97% of the membrane-bound protein was in the trimeric state (*19*). Because the EPR spectrum of 134R1 annexin A5 is very similar to that of 132R1 annexin B12, we conclude that a similar percent of membrane-bound annexin A5 forms a trimer. A trimer of annexin A5 previously had been detected by electron microscopy (*17*) and atomic force microscopy (*18*), but neither of those methods addressed the question of the percent of membrane-bound protein that was in the trimeric state.

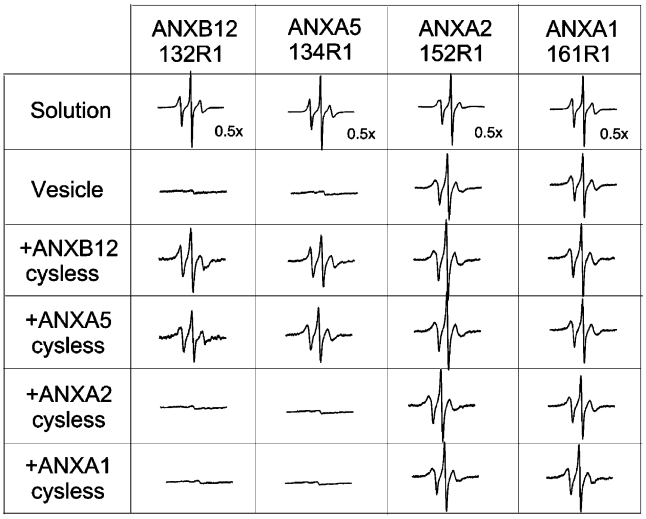

FIGURE 3: Evaluation of trimer formation by SDSL. Annexins A1, A2, A5, and B12 were labeled with R1 at the indicated positions. EPR spectra of these spin-labeled proteins were recorded in solution (top row) or following binding to PS/PC vesicles in the presence of Ca^{2+} (second row) as described in the Experimental Procedures. To evaluate the contribution of spin−spin coupling to the EPR spectra, spin-labeled annexins and unlabeled annexins were incubated with vesicles and Ca^{2+}. The bottom four rows present the entire matrix of mixing of labeled and unlabeled annexins (see the Experimental Procedures for details). The amplitudes of the spectra of proteins recorded in solution are reduced by half for ease of presentation. The spectral width is 100 G.

No spectral changes were noted for 134R1 annexin A5 and 132R1 annexin B12 when Ca^{2+} was added to solutions in the absence of vesicles (data not shown), thereby indicating that trimer formation was dependent on membranes.

As a further test of the assumption that the dramatic spectral changes observed for 132R1 annexin B12 and 134R1 annexin A5 were the results of multimer formation, unlabeled annexins were mixed with spin-labeled annexins prior to the addition of Ca^{2+} and vesicles. Assuming random assembly of labeled and unlabeled protein, spin−spin coupling within oligomers would be reduced because most oligomers would not contain two or more spin-labeled proteins. For example, when an excess of unlabeled annexin B12 was added to 132R1 annexin B12 (first panel in the third row of Figure 3), the EPR spectra were consistent with the R1 side chain located on a loop facing a central cavity in the trimer structure with little or no spin−spin interactions. Interestingly, unlabeled annexin B12 also had the same effect on 134R1 annexin A5 (second panel in the third row of Figure 3), thereby suggesting that annexins B12 and A5 form heterotrimers as previously noted (*19*). The addition of unlabeled annexin A5 to either 134R1 annexin A5 (second

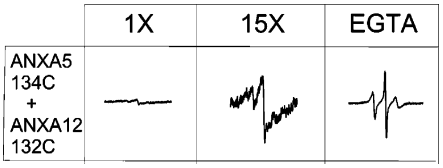

FIGURE 4: EPR analysis of annexins A5 and B12 heterotrimers. Equal amounts of 134R1 annexin A5 and 132R1 annexin B12 were bound to PS/PC vesicles in the presence of Ca^{2+}, and then the EPR spectra was recorded (left panel at 1× amplitude and center panel at 15× amplitude). EGTA was added to the same sample to chelate the Ca^{2+}, and the spectrum was again recorded (right panel at 1× amplitude). The spectral width is 100 G.

panel in the fourth row of Figure 3) or 132R1 annexin B12 (first panel in the fourth row of Figure 3) had the same effect as unlabeled annexin B12. Neither unlabeled annexin A5 nor B12 induced any observable change when added to either 152R1 annexin A2 or 161R1 annexin A1 (last two panels in the third and fourth rows of Figure 3). No observable changes were noted when either unlabeled annexin A2 or A1 were added to any of the four spin-labeled annexins. This observation supports the conclusion that neither annexin A2 nor A1 forms trimers and further indicates that these two annexins do not interfere with trimer formation by either annexin B12 or A5.

To directly determine whether annexins B12 and A5 form heterotrimers, equal amounts of 132R1 annexin B12 and 134R1 annexin A5 were mixed and allowed to bind to vesicles in the presence of Ca^{2+}. The EPR spectrum for this mixture (Figure 4) showed the same strong spin−spin coupling observed for the Ca^{2+}-dependent membrane-bound homotrimers of either annexin. After the addition of EGTA to the membrane-bound mixture of 132R1 annexin B12 and 134R1 annexin A5, the line shape of the EPR spectrum was consistent with monomers of these annexins in solution (Figure 4).

FRET Eperiments. As an independent measure of self-association of membrane-bound annexins, the same single-cysteine mutants used in the SDSL studies were labeled with Alexa 532 dye (fluorescence donor) and Alexa 647 dye (fluorescence acceptor) and used in FRET experiments (see the Experimental Procedures). In the experiments described herein, a qualitative assay was used that was based on the measurements of the excitation spectra in a mixture of donor- and acceptor-labeled annexins. FRET is considered to occur when excitation of the acceptor is observed near the absorption maxima of the donor dye (approximately 530 nm). When FRET was observed, one can conclude that the donor and acceptor probes were separated by a distance approximately equal to or less than the Förster distance for this pair, which is approximately 60 Å. If no FRET was observed, the separation between the dye pairs was significantly greater than this distance. Assuming that the minimal FRET efficiency that can be detected is 5%, the separating distance has to be more than 100 Å for FRET not to be observed in our experiments assuming that a single population exists.

Fluorescence excitation spectra for mixtures of donor- and acceptor-labeled annexins in the presence of PS/PC vesicles are shown in Figure 5. In the absence of Ca^{2+} to promote the association of the annexins with vesicles, all spectra (heavy trace in Figure 5) had spectral distributions that coincide with that of the pure acceptor dye (not shown). This means that there was no FRET under these conditions, consistent with a monomeric state of all four annexins in solution. Strong FRET-related signals were observed with a peak near 532 nm upon addition of Ca^{2+} to solutions

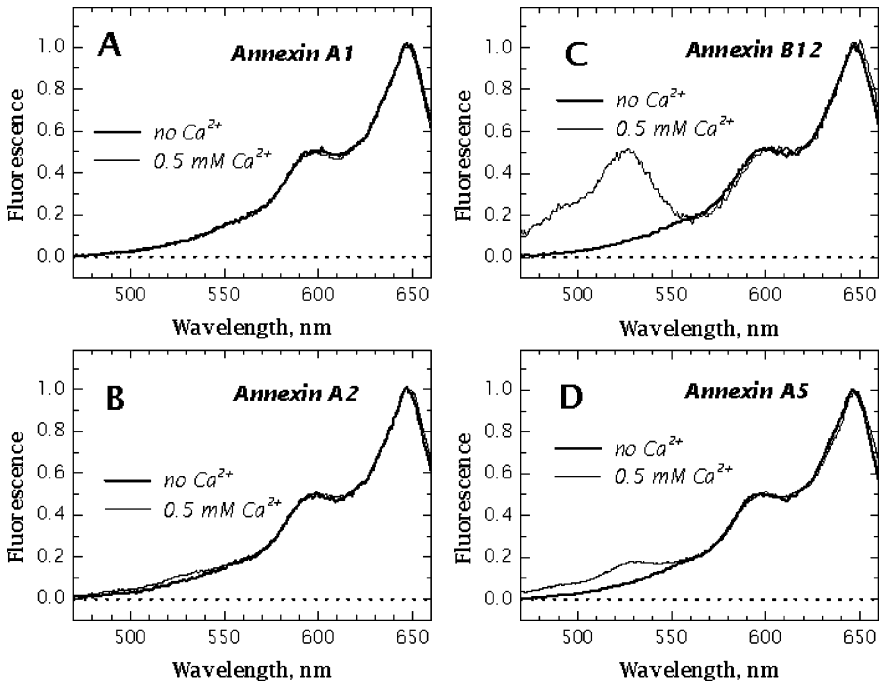

FIGURE 5: Fluorescence excitation spectra of donor- and acceptor-labeled annexin mutants. Single-Cys mutants of annexins A1, A2, A5, and B12 were labeled with either donor or acceptor dyes and then mixed in 1:2 molar ratios in a solution containing phospholipid vesicles in the absence (heavy trace) or presence (thin trace) of Ca^{2+} as described in the Experimental Procedures. The addition of Ca^{2+} triggers membrane association of all four annexins but results in the appearance of a FRET-related signal (donor peak at 530 nm) in the case of annexins A5 and B12 but not annexin A1 or A2. The Ca^{2+}-dependent FRET signal observed for annexins A5 and B12 was fully reversed by the addition of EGTA (data not shown).

containing vesicles and fluorescently labeled pairs of either annexin B12 or A5 (light trace in parts C and D of Figure 5). These FRET-related changes in the annexins B12 and A5 spectra were completely reversed by addition of EGTA (data not shown). In contrast, there was no significant FRET-related signal in the spectra of either labeled annexin A1 or A2 when membrane binding was induced by the addition of Ca^{2+} (light trace in parts A and B of Figure 5). A very slight change in the annexin 2 spectra in the 530 nm region was sometimes observed upon membrane binding (Figure 5B) perhaps by chance colocalization of donor- and acceptor-labeled annexin 2 in proximity with each other on the same vesicle. Fluorescence lifetime experiments are planned to quantitatively analyze the association of all four annexins; however, the results of these sensitive qualitative experiments presented in Figure 5 clearly indicate a high propensity for self-association of annexins A5 and B12 but not annexins A1 and A2.

Evaluation of Chimeras of Annexins A2 and A5. The core domains of all annexins have essentially the same backbone fold, and previous studies of a number of different annexins showed that it is possible to create stable and functional chimeras that have the N-terminal domain of one annexin and the core domain of a different annexin (*31*, *32*). As a first step toward determining whether the ability to form trimers resides in the variable N-terminal domain or the conserved core domain of annexins, we evaluated trimer formation of chimeras of annexins A2 and A5 in which their core and N-terminal domains were switched (see the Experimental Procedures). The chimeras that we created are called "2N-terminal:5core" and "5N-terminal:2core". Both chimeric proteins underwent reversible Ca^{2+}-dependent binding to phospholipid vesicles (data not shown).

The ability of these chimeric proteins to form trimers was analyzed indirectly using the SDSL strategy described in Figure 3. Unlabeled chimeric proteins were mixed with either 132R1 annexin B12 or 134R1 annexin A5, and then the mixture was added to vesicles in the presence of Ca^{2+}. If the unlabeled chimeric protein formed heterotrimers with the R1-labeled annexins, spin−spin coupling of the spin-labeled proteins would be disrupted and a distinctive EPR line shape would be produced. Figure 6 shows that the "2N-terminal:5core" chimera was as effective as either native annexin A5 or B12 in disrupting the spin−spin coupling observed with either 132R1 annexin B12 or 134R1 annexin A5. In contrast, the EPR spectra of both 132R1 annexin B12 and 134R1 annexin A5 were essentially the same in the presence or absence of the "5N-terminal:2core" chimera (Figure 6), thereby indicating that this chimera cannot form heterotrimers with either R1-labeled annexin. In summary, a comparison of native annexins A2 and A5 and the chimeric proteins indicated that the core domain mediated trimer formation. These experiments found no evidence that trimer formation was influenced to a detectable extent by the N-terminal domains.

Stoichiometry Measurements with $^{45}Ca^{2+}$ Copelleting Assay. Previous studies from a number of laboratories produced widely varying reports of Ca^{2+} stoichiometry of membrane-bound annexins (*33*−*36*). Many of the earlier studies of annexin Ca^{2+} stoichiometry employed equilibrium dialysis using $^{45}Ca^{2+}$, a method that presents problems for analyzing annexin Ca^{2+} binding. The main cause of the problems is high levels of background radioactivity in the experiments because the amount of $^{45}Ca^{2+}$ required to saturate annexin binding is high ($\geq 10^{-5}$ M) relative to the concentration of annexin that can be used and because negatively charged phospholipid bilayers have significant affinity for Ca^{2+}. To overcome these and other technical problems, we recently developed $^{45}Ca^{2+}$ copelleting and ITC methods and used them to study annexin B12. We now have used these methods to investigate the Ca^{2+}-binding stoichiometry of annexins A1, A2, and A5 to PS/PC phospholipid vesicles.

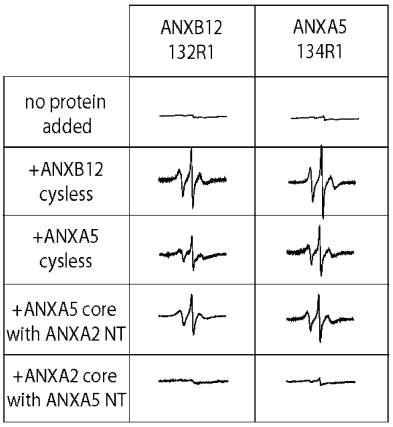

FIGURE 6: EPR analysis of annexin chimeras. The top row shows the EPR spectra of 132R1 annexin B12 and 134R1 annexin A5 while bound to PS/PC vesicles in the presence of Ca^{2+} as described in the Experimental Procedures. The other four rows show the entire matrix of mixing of 132R1 annexin B12 and 134R1 annexin A5 with either Cys-less annexin B12, Cys-less annexin A5, "2N-terminal:5core", or "5N-terminal:2core" as described in the Experimental Procedures. All unlabeled proteins except the "5N-terminal:2core" chimera disrupted spin−spin coupling of the nitroxide-labeled annexins as evidenced by the presence of the sharp central resonance line. This indicates that the "2N-terminal:5core" chimera but not the "5N-terminal:2core" chimera formed heterotrimers with the nitroxide-labeled annexins.

Table 1: Ca^{2+}-Dependent Binding of Annexins to Phospholipid Vesicles[a]

ANX	Ca^{2+} (μM)	stoichiometry	standard deviation (*n*)
A1	50	4.5	0.5 (4)
A2	25	1.6	0.3 (4)
A5	150	9.0	1.1 (6)
B12	150	11	0.4 (8)

[a] Each annexin (50 μg) was incubated with the indicated concentration of $^{45}Ca^{2+}$ and PS/PC phospholipid vesicles (1:5 ratio of protein/phospholipid by weight) as described in the Experimental Procedures. Ca^{2+}-binding stoichiometry (moles of Ca^{2+} per mole of annexin monomer) was determined in the copelleting assay described in the Experimental Procedures.

In the $^{45}Ca^{2+}$ copelleting assay, annexins and vesicles were incubated in the presence of $^{45}Ca^{2+}$ at a concentration that was approximately 5-fold higher than the concentration of Ca^{2+} required for half-maximal binding for each annexin under these conditions. Stoichiometries of 4.5 ± 0.5 mol of Ca^{2+}/mol of annexin A1, 1.6 ± 0.3 mol of Ca^{2+}/mol of annexin A2, and 9.0 ± 1.1 mol of Ca^{2+}/mol of annexin A5 were determined (Table 1). For comparison, the stoichiometry for annexin B12 in parallel assays was 9.2 ± 0.4, a value similar to that previously published (*24*).

ITC. The interaction of annexins A1, A2, and A5 with Ca^{2+} and PS/PC vesicles was studied by ITC at 25 °C.

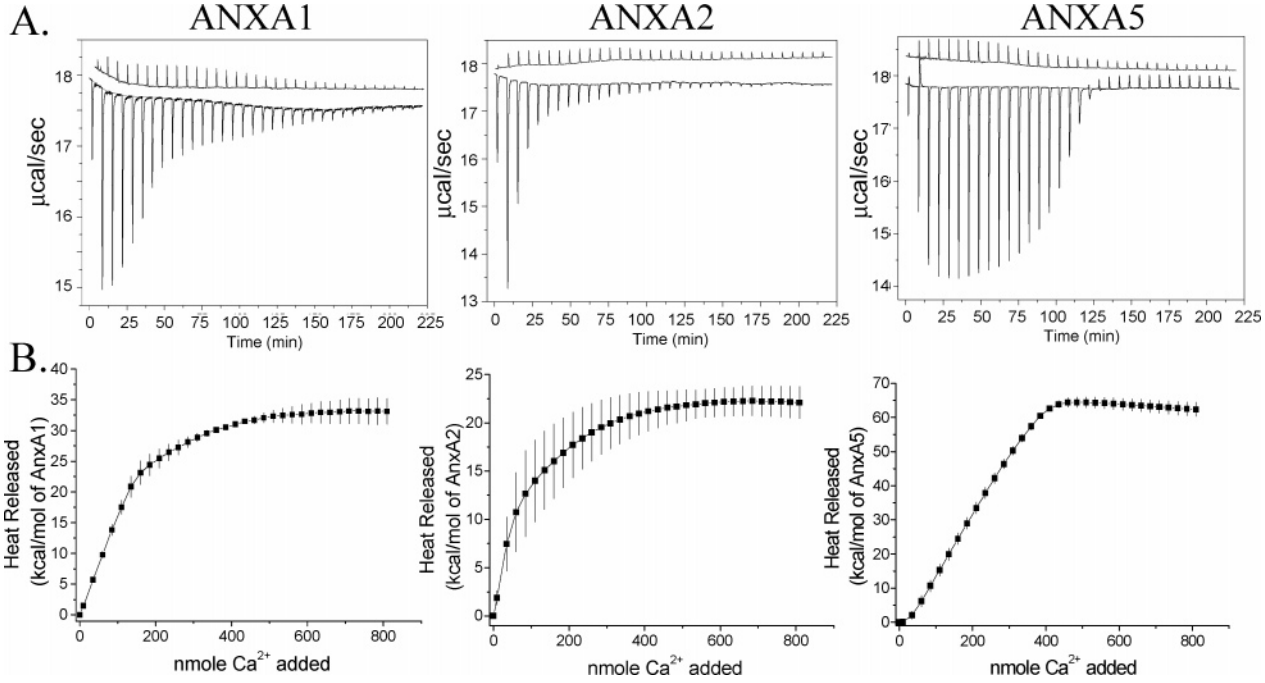

FIGURE 7: Isothermal calorimetric titration of annexins with Ca^{2+}. (A) PS/PC vesicles were titrated with $CaCl_2$ in the presence (lower trace) or absence (upper trace, offset) of annexin as described in the Experimental Procedures. Each titration event resulted in a downward (or upward) spike indicating the release (or absorption) of heat. The data in A are typical of two experiments, while data in B reflect an average of two experiments, with the error bars representing the standard deviation between the two experimental data sets. The raw data in A was integrated, and the heat change in the absence of annexin was subtracted from the heat change in the presence of the protein. (B) Cumulative annexin-specific heat release as a function of Ca^{2+} added. The curves for cumulative annexin-specific heat release for annexins A1 and A2 contained exponential and linear components, and the curves were fit using the equation: $y = A_1(1 - \exp(-x/x_1)) + mx$, where A_1 is the maximum heat released, x_1 is the nmoles of Ca^{2+} added, and m is the slope of the linear component. The R^2 values for these fits were 0.998 for annexin A1 and 0.996 for annexin A2. The linear component corresponded to 12 and 21% of the heat released at the high Ca^{2+} concentration for annexins A1 and A2, respectively. This linear component was subtracted from the curves of annexins A1 and A2 in B and used to calculate the Ca^{2+}-binding stoichiometry. The Ca^{2+}-binding stoichiometry for annexin A5 was calculated as previously described for annexin B12 (*24*).

Control experiments in which Ca^{2+} was titrated into a sample cell containing annexin and buffer did not detect any heat released (not shown). These results were expected because it is well-known that annexins have low affinity for Ca^{2+} in the absence of bilayers. When PS/PC vesicles were titrated with Ca^{2+} in the absence of annexins, relatively small upward spikes indicated a low amount of heat released over time after each titration event (upper traces of Figure 7A). When PS/PC vesicles were titrated with Ca^{2+} in the presence of either of the three annexins, larger downward spikes indicated a high amount of heat released (lower traces of Figure 7A). Figure 7B shows cumulative annexin-specific heat released as a function of Ca^{2+} added and was obtained by subtracting the control from the experimental data shown in Figure 7A. Analysis of the data in Figure 7B for annexin A5 was performed as previously described for annexin B12 (*24*). Briefly, the titration curve for annexin A5 describes a reaction that has three stages. The first stage included the initial two injections, which are reflective of partial binding of annexin A5 to the vesicles, while the Ca^{2+} concentration remained below that required for complete binding. Subsequently, a second stage of highly exothermic binding events of similar magnitude occurred, which was consistent with most of the added Ca^{2+} being sequestered by the binding of annexin A5 to the vesicles. In the third stage, each additional titration event resulted in a progressively reduced heat response as the Ca^{2+} sites reached saturation. Analysis of the annexin A5 titration curve indicated a stoichiometry of 12.0 ± 0.5 mol of Ca^{2+} bound/mol of annexin A5 monomer, with the entire binding process being complete after the addition of ~400 nmol of Ca^{2+}. This interpretation of the annexin A5 ITC data was consistent with parallel copelleting experiments that evaluated the annexin A5 vesicle association as a function of Ca^{2+} added (data not shown). The cumulative heat released for the formation of the ternary complex (annexin A5−Ca^{2+}−lipid) was -64.3 ± 0.4 kcal/mol annexin A5 (Figure 7B). A comparison of this study of annexin A5 with a previous study of annexin B12 (*24*) showed that both proteins had similar Ca^{2+}-binding stoichiometry and a similar highly exothermic nature.

In contrast to the ITC data for annexin A5 (Figure 7A) and annexin B12 (*24*), experiments with either annexin A1 or A2 showed that the first few additions of Ca^{2+} elicited the highest heat released (Figure 7A). It is reasonable to have the highest heat response within the first additions of Ca^{2+} for annexins A1 and A2 because they have higher affinity for Ca^{2+} than annexin A5 (*33*−*35*). Figure 7B shows cumulative annexin-specific heat released as a function of Ca^{2+} added after subtracting a minor linear component from the curve (see the caption of Figure 7). The nature of the linear component is not known, but it clearly did not saturate at Ca^{2+} concentrations that were much higher than those required to promote the proteins to bind to membranes. After the minor linear component was subtracted from the titration curves of annexins A1 and A2, the Ca^{2+}-binding stoichiometry was determined to be 4.1 ± 0.2 and 2.0 ± 0.1 mol of Ca^{2+}/mol of protein for annexins A1 and A2, respectively, and the cumulative heat released for the formation of the

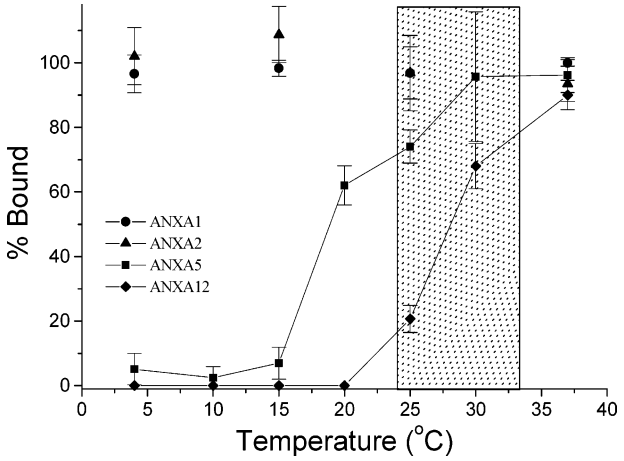

FIGURE 8: Annexin binding to lipids at the phase transition temperature. Phospholipid vesicles composed of PC and PS containing saturated acyl chains (DTPC and DMPS) were incubated with annexin A1, A2, or A5 at the indicated temperature (see the Experimental Procedures). Duplicate samples were analyzed to determine whether the annexins would copellet with the vesicles during centrifugation. The percentage of added annexin that associated with the pellet is shown along with the standard deviation of triplicate samples. The gray box indicates the phospholipid phase transition temperature range as determined experimentally by differential-scanning calorimetry in 100 mM HEPES buffer at pH 7.4. Control experiments carried out under the same conditions at 4 °C showed that annexins A1, A2, and A5 bound nearly quantitatively to vesicles composed of PS/PC that contained unsaturated acyl chains and remain in the liquid-crystal state at 4 °C.

ternary complex was -33.4 ± 0.5 kcal/mol for annexin A1 and -22.3 ± 1.2 kcal/mol for annexin A2. Clearly, the stoichiometry and enthalpy of Ca^{2+} binding are significantly different for annexins A1 and A2 compared to annexins A5 and B12. Similar results also were obtained when the experiments were performed in TRIS buffer.

We obtained Ca^{2+} stoichiometry values of ~4 and ~2 for annexins A1 and A2, respectively (Figure 7 and Table 1). Because experimental signals were lower with annexins A1 and A2, we think the estimates of their stoichiometry values are less accurate that those for annexins A5 and B12. Therefore, we do not attach much significance to the differences between the stoichiometry values obtained for annexins A1 and A2. Both of our values are in the same general range as most previous studies of these proteins (*34*, *37*). The important point that we want to stress is that there is a striking difference between the Ca^{2+} stoichiometry values determined for annexins A1 and A2 verses annexins A5 and B12.

Effects of Phospholipid-Bilayer Fluidity on Annexin Binding. Previous studies showed that the physical state of bilayers had a profound effect on the Ca^{2+}-dependent binding of annexin B12 (*24*). To extend these studies to annexins A1, A2, and A5, we prepared vesicles from phospholipids containing saturated acyl chains; therefore, the fluidity of the bilayer could be modulated by temperature in the physiological range. Vesicles composed of equal parts DMPS (14:0) and DTPC (13:0) underwent a phase transition from the liquid-crystal (fluid) to the gel phase in the 24−33 °C temperature range (gray box of Figure 8). Preliminary experiments showed that at 37 °C the Ca^{2+}-binding curves for annexins A1, A2, and A5 binding to these vesicles (data not shown) were indistinguishable from binding to vesicles composed of PS/PC from biological sources that have been used in our previous studies (*19*). In the presence of saturating Ca^{2+}, annexins A1, A2, and A5 bound nearly quantitatively to DMPS/DTPC vesicles at 37 °C (Figure 8). The temperature-dependent binding curve (Figure 8) shows that at all temperatures measured, annexins A1 and A2 maintained quantitative binding. In contrast, less than 10% of the added annexin A5 bound to vesicles when the temperature was below 20 °C. Even high concentrations of Ca^{2+} (500 μM) did not significantly increase the binding of annexin A5 to DMPS/DTPC vesicles at 4 °C (data not shown). Additionally, control experiments carried out under the same conditions at 4 °C show near quantitative binding of annexin A5 to vesicles composed of equal parts egg PC and brain PS, which contain unsaturated acyl chains and remain in the liquid-crystal phase at 4 °C (data not shown).

DISCUSSION

Although all of the biological functions of annexins have not been clearly defined, it is widely assumed that each of the many annexin gene products have different functional properties. These functional differences are often attributed to the structurally unrelated N-terminal domains, and there is compelling evidence that this is true for certain annexin functions. However, our current study adds support to the idea that important functional differences can also reside in the conserved core domain of this super family. We present evidence that there are at least two different groups of annexins that share distinctive common properties within each group. The defining characteristic of the two groups is whether the annexins could form trimers when they bound to bilayers in the presence of Ca^{2+}.

SDSL and FRET studies both detected self-association of membrane-bound annexins A5 and B12 (Figures 3 and 5). The strong interactions between the spin labels in the SDSL study indicated that the R1 side chains were in close proximity and provided compelling evidence that these proteins formed trimers on the bilayer that closely resembled the trimers observed in crystal structures of the soluble forms of these proteins (*14*, *15*). Over 97% of the membrane-bound annexins A5 and B12 formed trimers. Even though human annexin A5 and hydra annexin B12 are not orthologues, the two proteins readily combined to form heterotrimers *in vitro* (Figures 3 and 5). Considering the huge evolutionary distance between humans and hydra, it appears that the ability to form Ca^{2+}-dependent trimers was acquired early in annexin evolution.

In contrast to annexins A5 and B12, neither SDSL nor FRET studies of annexins A1 and A2 produced evidence for trimer formation (Figures 3 and 5). Because the maximum distance across the annexin monomer is shorter than the length of the FRET "molecular ruler" provided by our donor/acceptor dye pair, it is unlikely that any type of significant self-association of either annexin A1 or A2 occurred under the conditions of our experiments in which the annexins occupied approximately 1% of the surface of the vesicles (Figure 5). Of course, one would expect that densely packed areas of annexins A1 and A2 could occur if membranes were incubated with high concentrations of these proteins and, in fact, evidence of self-association of annexins A1 and A2 has

been presented (*38*−*40*). Evidence that annexins A1 and A2 are densely packed at membrane junctions following annexin-induced vesicle aggregation (*38*) is of particular interest and potential biological relevance. However, the structural mechanism by which annexins induce aggregation is not known. Significant data support the idea that the amino terminal domains of annexins A1 and A2 are involved in vesicle aggregation and suggest that structural components responsible for membrane binding may be different from those responsible for aggregation (*32*, *41*−*44*). In our current study, experimental conditions were optimal for low-density membrane binding but supported only minimal vesicle aggregation. Under the conditions of our experiments, it is clear that lateral self-association of annexins A1 and A2 did not occur to any significant extent. These results clearly show that oligomerization of membrane-bound annexins A1 and A2 is not a high-affinity event and is not important for inducing vesicle aggregation.

As a first step toward determining the structural mechanism of trimer formation, we constructed chimeras in which the N-terminal and core domains were swapped between annexin A5, which forms trimers, and annexin A2, which does not form trimers. The chimera with the annexin A5 core domain formed heterotrimers with R1-labeled annexins A5 and B12, but the chimera with the annexin A2 core domain could not form heterotrimers (Figure 6). Thus, the ability to form trimers resides in the core domain even though the core domains of annexins A1, A2, A5, and B12 all share ∼50% amino acid identity and have essentially identical backbone folds. In an attempt to recognize structural elements at the interface between protein monomers that would stabilize the trimer, we scanned the structures of the crystallographic trimers of annexins A5 and B12. The most obvious candidates were three salt bridges between the lateral edges of adjacent annexin B12 monomers (*14*). Annexin A5 trimers had two salt bridges at locations homologous to those in annexin B12 (*15*). In contrast, with only a single exception, the amino acids at homologous locations in annexins A1 and A2 were not suitable for salt-bridge formation. Although these salt bridges appear to be good candidates for protein/protein interactions that stabilize membrane-bound trimers, we found that mutation of all three of these sites in annexin B12 did not disrupt Ca^{2+}-dependent trimer formation on membranes (our unpublished results). Thus, the role, if any, played by these salt bridges must be minor. Because there are no other obvious candidates for significant protein/protein contact sites that stabilize the trimer, it appears that the interaction with phospholipid plays the major role in inducing trimer formation.

The two annexins that formed trimers in our study had Ca^{2+}-dependent membrane-binding properties that were distinctly different from the two annexins that did not form trimers. Trimer-forming annexins A5 and B12 had a much higher Ca^{2+} stoichiometry for membrane binding (∼12 mol of Ca^{2+}/mol of protein monomer) than annexins A1 and A2 (≤4 mol of Ca^{2+}/mol of protein). Several of the amino acids involved in formation of Ca^{2+}-binding sites in annexins A5 and B12 are missing in annexins A1 and A2, thereby providing at least a partial structural explanation for the differences in Ca^{2+} stoichiometry. The clear differences in Ca^{2+} stoichiometry values may be responsible for previously reported Ca^{2+}-dependent membrane-binding properties of these annexins. Annexins A5 and B12 have remarkably cooperative curves for membrane binding as a function of the Ca^{2+} concentration with Hill constants of up to ∼7 (*24*, *45*). In contrast, Ca^{2+}-dependent membrane binding of annexins A1 and A2 is not cooperative (*34*, *37*). Thus, annexins A5 and B12 appear better suited for an all-or-none type of response to rising cellular Ca^{2+} concentrations.

As previously reported for annexin B12 (*24*), Ca^{2+}-dependent membrane binding of annexin A5 is very exothermic ($\Delta H = -64$ kcal/mol protein). In contrast, binding of annexins A1 and A2 was relatively less exothermic ($\Delta H < -33$ kcal/mol protein). These data do not imply that the ΔG values for the two pairs of proteins are strikingly different because one would expect the entropic contribution to be much higher for the trimer-forming annexins. In addition to the entropic contributions from trimer assembly and high Ca^{2+} binding, these proteins also appear to immobilize the phospholipid headgroups with which they interact (*12*, *46*).

We previously showed that annexin B12 lost the ability to bind to vesicles when the bilayers underwent a phase transition from the liquid-crystal to the gel phase (*24*). We speculated that there is a complimentarity between the spacing of the Ca^{2+}-binding sites on annexin B12 and the spacing of the headgroups of phospholipids in liquid-crystal bilayers and that this complimentarity is lost when the density of the bilayer increases as it transitions from the liquid-crystal phase to the gel phase. Studies reported herein showed that annexin A5 behaved like annexin B12 and did not bind to bilayers that were in the gel phase (Figure 8). In contrast, annexins A1 and A2 bind with high affinity to bilayers in either physical state (Figure 8). This *in vitro* data implies that in biological settings annexins A5 and B12 interact extensively with membranes and immobilize the phospholipid headgroups, while annexins A1 and A2 have more limited interactions and do not immobilize the lipid. In support of this speculation, recent electrophysiological studies showed that annexins A5 and B12 prevent "flip-flop" of bilayer phospholipids but annexins A1 and A2 have minimal effect on flip-flop (Sokolov, Y., Hall, J., Haigler, H. T., Isas, J. M., and Langen, R., unpublished results).

One theme that emerges from this and other studies of annexins is the structural and functional importance of the interaction between the protein and phospholipid bilayer. In general, a variety of different proteins oligomerize following association with membranes, and it often is assumed that the increased concentration of protein in the plane of the bilayer drives the protein/protein association. However, the current study showed that specific interactions between bilayers and annexins A5 and B12 were involved in inducing trimer formation. Trimer formation was not observed in solution even at very high protein and Ca^{2+} concentrations. Furthermore, a particular physical state of the bilayer was required for annexins A5 and B12 trimer formation. This study raises the possibility that quaternary changes in other proteins could be induced by specific interactions with phospholipid bilayers.

Previous studies showed that annexins A5 and B12 immobilize the headgroups of phospholipids with which they interact (*24*, *46*). Both proteins form extended 2D crystals of trimers (*17*, *18*, and our unpublished results) and thus have the potential to act as molecular fences that restrict the diffusion of other membrane proteins. Because previous

studies showed that annexin A4 also forms Ca^{2+}-dependent membrane-bound trimers (*16*) and immobilizes membrane lipids (*47*), it will be particularly interesting to determine whether it shares other properties with annexins A5 and B12. Furthermore, because annexins A4 and A5 are coexpressed in many mammalian cells, it is possible that they form heterotrimers, which would introduce another type of Ca^{2+}-dependent regulation by annexins. If annexin trimers immobilize the fluidity of cellular membranes, Ca^{2+}-dependent trimer formation could participate in creating or maintaining the nonrandom distribution of membrane proteins. The possibility that this is a physiological function of trimer-forming annexins is supported by a recent *in vitro* study showing that annexin B12 dramatically reduced the lateral diffusion coefficient of the ryanodine receptor in bilayers without altering its conductance properties (*48*). In contrast to annexins A5 and B12, annexins A1 and A2 do not form trimers, have significantly fewer Ca^{2+}-binding sites, and have not been reported to immobilize phospholipid headgroups. Thus, annexins A1 and A2 do not appear to be well-suited to alter the bilayer structure as a biological function. We speculate that their Ca^{2+}-dependent membrane-binding activity may be a zip code that directs them to sites of action such as near vesicle fusion sites. Additional experiments are needed to determine whether the trimer-based grouping will apply to other annexin gene products and whether this approach will help to explain the mechanism by which different annexin gene products are targeted to different subcellular locations.

REFERENCES

1. Moss, S. E., and Morgan, R. O. (2004) The annexins, *Genome Biol. 5*, 219.
2. Gerke, V., and Moss, S. E. (2002) Annexins: From structure to function, *Physiol. Rev. 82*, 331−371.
3. Rescher, U., and Gerke, V. (2004) Annexins—Unique membrane binding proteins with diverse functions, *J. Cell Sci. 117*, 2631−2639.
4. Christmas, P., Callaway, J., Fallon, J., Jones, J., and Haigler, H. T. (1991) Selective secretion of annexin 1, a protein without a signal sequence, by the human prostate gland, *J. Biol. Chem. 266*, 2499−2507.
5. Langen, R., Isas, J., Hubbell, W., and Haigler, H. (1998) A transmembrane form of annexin XII detected by site-directed spin labeling, *Proc. Natl. Acad. Sci. U.S.A. 95*, 14060−14065.
6. Kohler, G., Hering, U., Zschoring, O., and Arnold, K. (1997) Annexin V interaction with phosphatidylserine-containing vesicles at low and neutral pH, *Biochemistry 36*, 8189−8194.
7. Seaton, B. A. (1996) *Annexins: Molecular Structure to Cellular Function* (Seaton, B. A., Ed.) R. G. Landes Company, Austin, TX.
8. Isas, J. M., Patel, D. R., Jao, C., Jayasinghe, S., Cartailler, J. P., Haigler, H. T., and Langen, R. (2003) Global structural changes in annexin 12. The roles of phospholipid, calcium, and pH, *J. Biol. Chem. 278*, 30227−30234.
9. Oh, P., Li, Y., Yu, J., Durr, E., Krasinska, K. M., Carver, L. A., Testa, J. E., and Schnitzer, J. E. (2004) Subtractive proteomic mapping of the endothelial surface in lung and solid tumours for tissue-specific therapy, *Nature 429*, 629−635.
10. Rand, J. (1999) "Annexinopathies"—A new class of diseases [editorial; comment], *N. Engl. J. Med. 340*, 1035−1036.
11. Menell, J., Cesarman, G., Jacovina, A., McLaughlin, M., Lev, E., and Hajjar, K. (1999) Annexin II and bleeding in acute promyelocytic leukemia, *N. Engl. J. Med. 340*, 994−1004.
12. Isas, J. M., Langen, R., Hubbell, W. L., and Haigler, H. T. (2004) Structure and dynamics of a helical hairpin that mediates calcium-dependent membrane binding of annexin B12, *J. Biol. Chem. 279*, 32492−32498.
13. Swairjo, M. A., Concha, N. O., Kaetzel, M. A., Dedman, J. R., and Seaton, B. A. (1995) Ca^{2+}-bridging mechanism and phospholipid head group recognition in the membrane-binding protein annexin V, *Nat. Struct. Biol. 2*, 968−974.
14. Luecke, H., Chang, B. T., Mailliard, W. S., Schlaepfer, D. D., and Haigler, H. T. (1995) Crystal structure of the annexin XII hexamer and implications for bilayer insertion, *Nature 378*, 512−515.
15. Mo, Y., Campos, B., Mealy, T. R., Commodore, L., Head, J. F., Dedman, J. R., and Seaton, B. A. (2003) Interfacial basic cluster in annexin V couples phospholipid binding and trimer formation on membrane surfaces, *J. Biol. Chem. 278*, 2437−2443.
16. Kaetzel, M. A., Mo, Y. D., Mealy, T. R., Campos, B., Bergsma-Schutter, W., Brisson, A., Dedman, J. R., and Seaton, B. A. (2001) Phosphorylation mutants elucidate the mechanism of annexin IV-mediated membrane aggregation, *Biochemistry 40*, 4192−4199.
17. Oling, F., Santos, J. S., Govorukhina, N., Mazeres-Dubut, C., Bergsma-Schutter, W., Oostergetel, G., Keegstra, W., Lambert, O., Lewit-Bentley, A., and Brisson, A. (2000) Structure of membrane-bound annexin A5 trimers: A hybrid cryo-EM−X-ray crystallography study, *J. Mol. Biol. 304*, 561−573.
18. Reviakine, I., Bergsma-Schutter, W., Mazeres-Dubut, C., Govorukhina, N., and Brisson, A. (2000) Surface topography of the p3 and p6 annexin V crystal forms determined by atomic force microscopy, *J. Struct. Biol. 131*, 234−239.
19. Langen, R., Isas, J. M., Luecke, H., Haigler, T. H., and Hubbell, W. L. (1998) Membrane-mediated assembly of annexins studied by site-directed spin labeling, *J. Biol. Chem. 273*, 22453−22457.
20. Isas, J. M., Langen, R., Haigler, H. T., and Hubbell, W. L. (2002) Structure and dynamics of a helical hairpin and loop region in annexin 12: A site-directed spin labeling study, *Biochemistry 41*, 1464−1473.
21. McHaourab, H. S., Lietzow, M. A., Hideg, K., and Hubbell, W. L. (1996) Motion of spin-labeled side chains in T4 lysozyme. Correlation with protein structure and dynamics, *Biochemistry 273*, 810−812.
22. Columbus, L., and Hubbell, W. L. (2002) A new spin on protein dynamics, *Trends Biochem. Sci. 27*, 288−295.
23. Montaville, P., Neumann, J. M., Russo-Marie, F., Ochsenbein, F., and Sanson, A. (2002) A new consensus sequence for phosphatidylserine recognition by annexins, *J. Biol. Chem. 277*, 24684−24693.
24. Patel, D. R., Jao, C. C., Mailliard, W., Isas, J., Langen, R., and Haigler, H. (2001) Calcium-dependent binding of annexin 12 to phospholipid bilayers: Stoichiometry and implications, *Biochemistry 40*, 7054−7060.
25. Rosengarth, A., Rösgen, J., Hinz, H. J., and Gerke, V. (1999) A comparison of the energetics of annexin I and annexin V, *J. Mol. Biol. 288*, 1013−1025.
26. Kirsch, T., Harrison, G., Golub, E. E., and Nah, H. D. (2000) The roles of annexins and types II and X collagen in matrix vesicle-mediated mineralization of growth plate cartilage, *J. Biol. Chem. 275*, 35577−35583.
27. Kirsch, T., Nah, H. D., Demuth, D. R., Harrison, G., Golub, E. E., Adams, S. L., and Pacifici, M. (1997) Annexin V-mediated calcium flux across membranes is dependent on the lipid composition: Implications for cartilage mineralization, *Biochemistry 36*, 3359−3367.
28. Reeves, J. P., and Dowben, R. M. (1969) Formation and properties of thin-walled phospholipid vesicles, *J. Cell. Physiol. 73*, 49−60.
29. Haugland, R. P. (1996) *Handbook of Fluorescent Probes and Research Chemicals*, Molecular Probes, Inc., Eugene, OR.
30. Ladokhin, A. S., Jayasinghe, S., and White, S. H. (2000) How to measure and analyze tryptophan fluorescence in membranes properly, and why bother? *Anal. Biochem. 285*, 235−245.
31. Konig, J., and Gerke, V. (2000) Modes of annexin−membrane interactions analyzed by employing chimeric annexin proteins, *Biochim. Biophys. Acta 1498*, 174−180.
32. Bitto, E., and Cho, W. (1999) Structural determinant of the vesicle aggregation activity of annexin I, *Biochemistry 38*, 14094−14100.
33. Glenney, J. (1986) Phospholipid-dependent Ca^{2+} binding by the 36-kDa tyrosine kinase substrate (calpactin) and its 33-kDa core, *J. Biol. Chem. 261*, 7247−7252.
34. Schlaepfer, D. D., and Haigler, H. T. (1987) Characterization of Ca^{2+}-dependent phospholipid binding and phosphorylation of lipocortin I, *J. Biol. Chem. 262*, 6931−6937.
35. Schlaepfer, D. D., Mehlman, T., Burgess, W. H., and Haigler, H. T. (1987) Structural and functional characterization of endonexin II, a calcium- and phospholipid-binding protein, *Proc. Natl. Acad. Sci. U.S.A. 84*, 6078−6082.

36. Evans, T. C., Jr., and Nelsestuen, G. L. (1994) Calcium and membrane-binding properties of monomeric and multimeric annexin II, *Biochemistry 33*, 13231−13238.
37. Jost, M., Weber, K., and Gerke, V. (1994) Annexin II contains two types of Ca^{2+}-binding sites, *Biochem. J.* (Part 3) *298*, 553−559.
38. Lambert, O., Gerke, V., Bader, M., Porte, F., and Brisson, A. (1997) Structural analysis of junctions formed between lipid membranes and several annexins by cryo-electron microscopy, *J. Mol. Biol. 272*, 42−55.
39. Bitto, E., Li, M., Tikhonov, A. M., Schlossman, M. L., and Cho, W. (2000) Mechanism of annexin I-mediated membrane aggregation, *Biochemistry 39*, 13469−13477.
40. Janshoff, A., Ross, M., Gerke, V., and Steinem, C. (2001) Visualization of annexin I binding to calcium-induced phosphatidylserine domains, *ChemBioChem 2*, 587−590.
41. de la Fuente, M., and Parra, A. V. (1995) Vesicle aggregation by annexin I: Role of a secondary membrane binding site, *Biochemistry 34*, 10393−10399.
42. Johnstone, S. A., Hubaishy, I., and Waisman, D. M. (1992) Phosphorylation of annexin II tetramer by protein kinase C inhibits aggregation of lipid vesicles by the protein, *J. Biol. Chem. 267*, 25976−25981.
43. Johnstone, S. A., Hubaishy, I., and Waisman, D. M. (1993) Regulation of annexin I-dependent aggregation of phospholipid vesicles by protein kinase C, *Biochem. J. 294*, 801−807.
44. Wang, W., and Creutz, C. E. (1994) Role of the amino-terminal domain in regulating interactions of annexin I with membranes: Effects of amino-terminal truncation and mutagenesis of the phosphorylation sites, *Biochemistry 33*, 275−282.
45. Tait, J. F., Gibson, D. F., and Smith, C. (2004) Measurement of the affinity and cooperativity of annexin V-membrane binding under conditions of low membrane occupancy, *Anal. Biochem. 289*, 329.
46. Megli, F. M., Selvaggi, M., Liemann, S., Quagliariello, E., and Huber, R. (1998) The calcium-dependent binding of annexin V to phospholipid vesicles influences the bilayer inner fluidity gradient, *Biochemistry 37*, 10540−10546.
47. Gilmanshin, R., Creutz, C. E., and Tamm, L. K. (1994) Annexin IV reduces the rate of lateral lipid diffusion and changes the fluid phase structure of the lipid bilayer when it binds to negatively charged membranes in the presence of calcium, *Biochemistry 33*, 8225−8232.
48. Peng, S., Publicover, N. G., Airey, J. A., Hall, J. E., Haigler, H. T., Jiang, D., Chen, S. R., and Sutko, J. L. (2004) Diffusion of single cardiac ryanodine receptors in lipid bilayers is decreased by annexin 12, *Biophys. J. 86*, 145−151.

BI047642+